Interventional Digital Tomosynthesis from a Standard Fluoroscopy System Using 2D-3D Registration

Mazen Alhrishy[1], Andreas Varnavas[1], Tom Carrell[2], Andrew King[1], and Graeme Penney[1]

[1] Biomedical Engineering Dept., King's College London, London, UK*
[2] Vascular Surgery Dept., Guys & St Thomas' NHS Foundation Trust, London, UK

Abstract. Fluoroscopy is the mainstay of interventional radiology. However, the images are 2D and visualisation of vasculature requires nephrotoxic contrast. Cone-beam computed tomography is often available, but involves large radiation dose and interruption to clinical workflow. We propose the use of 2D-3D image registration to allow digital tomosynthesis (DTS) slices to be produced using standard fluoroscopy equipment. Our method automatically produces patient-anatomy-specific slices and removes clutter resulting from bones. Such slices could provide additional intraoperative information, offering improved guidance precision. Image acquisition would fit with interventional clinical workflow and would not require a high x-ray dose. Phantom results showed a 1133% contrast-to-noise improvement compared to standard fluoroscopy. Patient results showed our method enabled visualisation of clinically relevant features: outline of the aorta, the aortic bifurcation and some aortic calcifications.

Keywords: Interventional digital tomosynthesis, 2D-3D image registration, endovascular aneurysm repair.

1 Introduction

The fundamentals behind interventional fluoroscopy have remained largely unchanged since its inception. Large advances have been made in detector sensitivity, however, clinicians still view 2D projective "shadow" images which simply integrate all information along the beam path. This often results in clinically relevant information being obscured by over- or under-lying anatomy.

Enhancement of blood vessels using iodinated contrast is routine, but must be used sparingly as contrast is nephrotoxic. In modern fluoroscopy suites, 3D imaging is often available via semicircular C-arm rotation, i.e. cone beam CT (CBCT). However, the set-up time for CBCT (5∼10 min) can cause a large interruption to clinical workflow, especially if multiple acquisitions are required [8]. Repeated CBCT also involves a significant radiation dose [2]. In addition, the

* Thanks go to the King's Overseas Research Studentship scheme for funding.

K. Mori et al. (Eds.): MICCAI 2013, Part III, LNCS 8151, pp. 98–105, 2013.

3D nature of CBCT images requires some interaction from clinicians to scan through 2D sections to find the clinically relevant information. For these reasons, CBCT is not a natural interventional modality, and is unlikely to be used repeatedly during interventions to aid guidance.

Tomosynthesis was the first medical sectional modality, but was largely superseded by computed tomography after its invention in the 1970s. In the last decade, however, digital tomosynthesis (DTS) is being increasingly used for diagnosis of breast lesions and pulmonary nodules as it offers some of the tomographic benefits of CT but at substantially lower dose and shorter acquisition time [3]. Nevertheless, such diagnostic systems require dedicated equipment and suffer from the presence of background "clutter", caused by high contrast features outside the slice of interest.

Recently, a 3D DTS prototype system, based on a mobile isocentric C-arm, has been proposed for intraoperative guidance of head and neck surgery [1]. The limited DTS arc (e.g. $20° \sim 90°$) enabled a short acquisition time and low radiation dose causing minimal interruption to surgical workflow [2]. However, apart from being modified for intraoperative use, the prototype employs the same technique as diagnostic DTS systems and suffers from the same drawbacks.

In this submission, we propose the use of 2D-3D image registration to facilitate DTS as an interventional modality which allows repeated acquisitions and results in minimal interruption to standard clinical workflow. Moreover, we propose a method which: produces DTS slices using a standard fluoroscopy system; can automatically produce patient-anatomy-specific DTS slices that display the most clinically relevant information; and can automatically remove clutter resulting from bony anatomy.

2 Materials and Methods

DTS slice reconstruction requires a set of 2D intraoperative images to be acquired from a limited range of view directions. These are reconstructed into a sectional slice, commonly using the shift and add method, which combines the fluoroscopy images so that structures in the reconstruction plane line-up, and so appear in-focus, while structures outside the reconstruction plane are not aligned, and so are blurred-out.

2.1 DTS Required Information and Main Limitation

In order to reconstruct a DTS slice, the following is required:

1. Relative view positions of input 2D images.
2. Reconstruction plane position with respect to the imaging device.

Standard diagnostic DTS obtains relative view positions using mechanical tracking. This requires a calibration process, and calibration errors can result in artifacts and reduced image quality [6]. Also in standard diagnostic DTS, a number of slices are reconstructed on planes defined with respect to the imaging

device. Prior to reconstruction it is not possible to define a reconstruction plane to image specific regions of the patient's anatomy.

DTS attempts to blur-out all structures outside the reconstruction plane, but because of the limited data acquisition, clutter from high contrast structures above and below the reconstruction plane remain. A number of methods have been proposed to reduce the effect of clutter [4], but this remains one of the main problems of DTS [5].

2.2 Using 2D-3D Registration to Facilitate Enhanced DTS Using a Standard Fluoroscopy System

Our interventional DTS method uses an established intensity-based 2D-3D registration algorithm [7]. The novelty of this paper is with respect to the use of 2D-3D registration to facilitate improved DTS reconstruction using standard hardware, on patient-anatomy-specific surfaces and with reduced clutter.

Figure 1 shows an overview of the entire process. This begins at the top with the input images: a C-arm sweep (1) to produce a set (of size n) of intraoperative fluoroscopy images (2), and a preoperative CT scan (3). These images are input into the 2D-3D registration algorithm which calculates the 2D-3D transformations P_i between the CT scan and each of the n fluoroscopy images. The registration provides us with the necessary information to carry out DTS and enables us to greatly reduce clutter from bone. This is illustrated by the three boxes showing the output from the 2D-3D registration in Fig. 1, where the Roman numerals labelling each box correspond to the below descriptions:

I. Calculate view positions: The transformations P_i enable the relative view positions of the input 2D images to be determined.
II. Position reconstruction surface: A patient-anatomy-specific plane can be preoperatively defined in the CT scan. The transformations P_i can position this plane with respect to the fluoroscopy images, enabling reconstruction to occur on a patient-anatomy-specific plane.
III. Remove bones: Bony details from the CT scan in the form of digitally reconstructed radiographs (DRRs) can be produced for each fluoroscopy image using the transformations P_i. DRRs are produced by casting rays through automatically segmented vertebra from the CT and integrating voxel values above a threshold (200 HU). Therefore, DRR intensities come only from vertebral bone ((4).a). The DRR can be subtracted from the fluoroscopy image ((4).b) to give a "deboned" image ((4).c) leaving just the soft tissue and aortic calcifications (features of clinical interest), and any interventional instruments. This deboning process is carried out on each fluoroscopy image prior to reconstruction to greatly reduce clutter from high contrast bony features.

In addition, we propose the use of curved patient-anatomy-specific reconstruction surfaces. It is rare that structures of clinical interest lie on flat planes. Our aim in interventional DTS is to produce images with enhanced clinically relevant

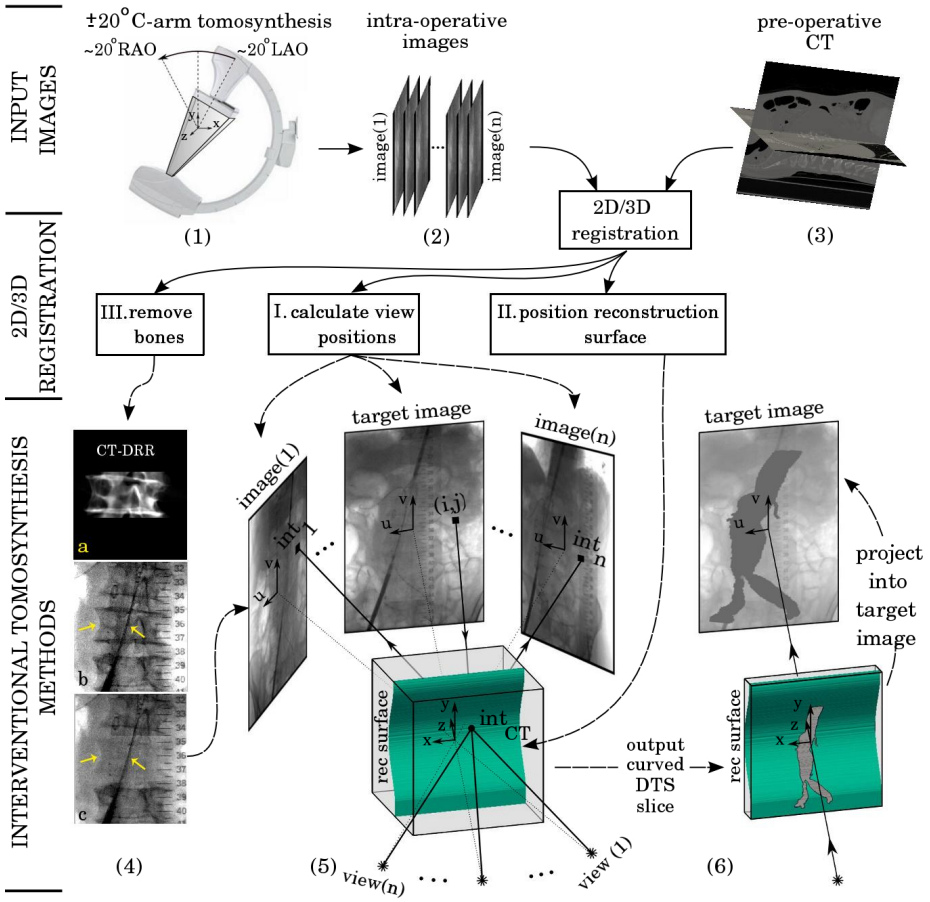

Fig. 1. A flow diagram of overall method. Top shows input images (intraoperative fluoroscopy images (1,2) and preoperative CT (3)). Middle shows the 2D-3D registration which enables bone removal (4), calculation of view directions and positioning of curved patient-anatomy-specific reconstruction surface. Bottom shows interventional DTS process producing the DTS slice containing additional clinical information (5) and then projection of this information into the fluoroscopy image to aid guidance (6).

structures. As shown in Fig. 2, if the structure of clinical interest is the aorta, then only approximately half of its length could be included in a flat reconstruction plane (Fig. 2.(a&b)). The use of a curved surface allows reconstruction of the entire length of the aorta (Fig. 2.(c&d)).

Returning to Fig. 1, the tomosynthesis process is shown in (5). Here, after bone removal and using the transformations P_i, rays are back projected from the target image onto the patient-anatomy-specific reconstruction surface (e.g. pixel (i, j)). Rays are then forward projected from 3D interception positions (e.g. $\mathrm{int}_{\mathrm{CT}}$) to each of the other images in turn. The intensity values from each

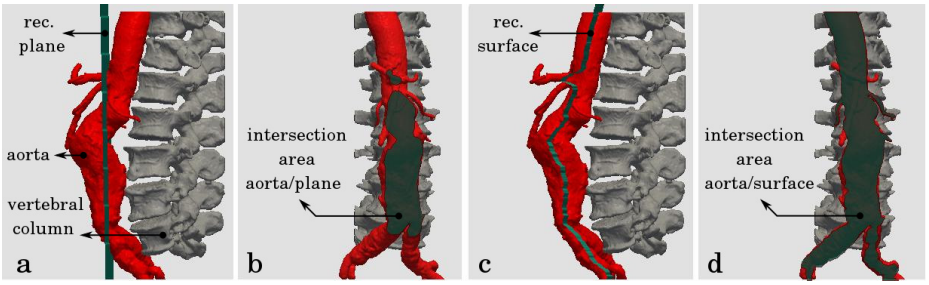

Fig. 2. Illustration of advantage of using curved surface over flat plane for DTS where aorta is feature of clinical interest: (a,c) sagittal views showing (a) flat reconstruction plane intersecting aorta and (c) curved reconstruction surface along aortic centreline; (b,d) anterior views showing (b) flat plane only intersects with roughly half of aorta whereas (d) curved surface can intersect (and therefore can reconstruct) entire aorta

2D interception position (e.g. $\text{int}_1, \ldots, \text{int}_n$) are summed to produce a curved patient-anatomy-specific DTS slice. In order to allow effective use of this new information, the reconstructed slice is then projected onto the target image being used to guide the operation (6). This automatically produces an enhanced fluoroscopy image which shows additional information of the clinical features of interest, in the view being clinically used.

3 Data and Experiments

Experiments were carried out using data from an abdominal spine phantom and from two patients who underwent endovascular aortic repair (approved by national research ethics committee (09/H0707/64)). Each data set had a pre-operative CT scan; and intraoperative low dose screening images acquired by rotating the C-arm $\sim 20°$ right/left anterior oblique with a frame rate of 30 fps, which were resampled to obtain one image per one degree of rotation, i.e. ~ 40 images. Set-up time for the $\sim 20°$ sweep took less than a minute for each data acquisition. For comparison, a series of ~ 40 screening images from an anterior-posterior view were also saved and averaged to produce a high contrast image from a single view direction.

The phantom CT had voxel sizes of $1.094 \times 1.094 \times 1.487\, mm^3$. Prior to fluoroscopy acquisition, an interventional instrument (a catheter) and three pieces of Blu-Tack (to represent calcium in the aortic wall) were placed on the anterior surface of the phantom. Therefore, the anterior surface of the CT volume was used for reconstruction.

The patients' standard diagnostic CT scans had voxel sizes of approximately $0.75 \times 0.75 \times 0.8\, mm^3$. The reconstruction surface was defined to intersect the curved aortic centreline and to be perpendicular to the sagittal plane. This surface was chosen to enhance features of interest such as the aortic walls.

DTS slice reconstruction, as described in Sec. 2.2, was carried out for both phantom and clinical data sets to reconstruct two interventional DTS slices, the

first using the standard fluoroscopy images, and the second using the fluoroscopy images after applying the deboning process. After providing a starting position for the first 2D-3D registration the registrations were totally automatic. As real data was used, our experiments included realistic registration errors.

For the phantom data set, the contrast-to-noise ratio (CNR) values were calculated on profile lines as follows: CNR $= (\bar{I}_{FG} - \bar{I}_{BG})/\sigma_{BG}$, where $\bar{I}_{FG}$ and $\bar{I}_{BG}$ were the mean foreground and background intensities, and σ_{BG} was the standard deviation in the background region.

For clinical data, CT segmentations were overlaid onto the DTS slices to provide context to the enhanced features. The first overlay shows the aorta, and the second shows aortic calcification. The overlay was initally positioned using the 2D-3D registration, and then due to intraoperative aortic deformation, the overlay was manually moved to match the aortic outline in the DTS slices.

4 Results

For each data set we show: the target image (TI), the high contrast image (CI), the reconstructed slice (DTS) and the reconstructed slice after deboning, i.e deboned DTS (DDTS). We also show the two CT overlays for the clinical data.

Figure 3 shows the phantom results. The high contrast catheter can be clearly seen in all images; whereas the low contrast synthetic calcium cannot be clearly distinguished in 'a' nor 'b' from the overlying vertebrae. However, in both DTS reconstructions, 'c' and 'd', the synthetic calcium is successfully brought into focus (indicated by circles). Significantly more clutter from the underlying vertebrae can be seen in 'c', compared to the reconstruction after deboning 'd'.

Table 1 shows CNR results, and percentage improvement in CNR compared to TI, calculated on the profile lines (PL) shown in Fig. 3. CNR values were calculated on three lines close to the PLs shown (one on the PL and two with the line vertically shifted by $\pm$ 3 pixels), and the results were averaged. Foreground region was defined as the region within FWHM calculated using the DDTS image (as features could be most clearly observed). PLs 1,2 and 3 are through synthetic calcium and PL4 is through the catheter. An average improvement of 72% is seen between TI and CI as random noise is averaged. Both DTS and DDTS show much improved CNR for the low contrast synthetic calcium and for the high contrast catheter, and the further improvement due to the deboning method is clearly seen.

Figure 4 shows the patient data results. Comparing the overlay outline in 'e' and 'd' shows how the DDTS method has been able to show the outline of the aorta. Some calcium deposits (indicated by arrows) were also enhanced, and for patient 1 the aortic bifurcation was visible. Comparison between 'c' and 'd' clearly show the benefits of the deboning process, and although 'b' shows a high contrast image of the instruments and bony anatomy, none of the clinically relevant soft tissue features enhanced by the DTS process are visible.

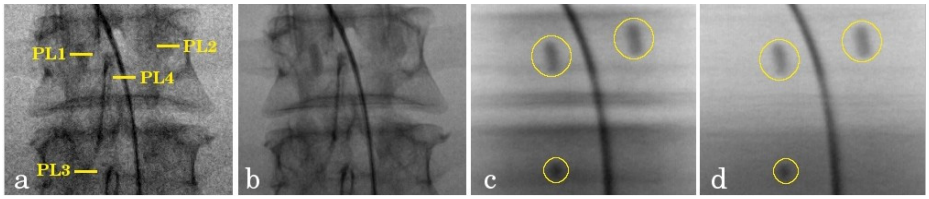

Fig. 3. Phantom results: a) TI with profile lines positions, b) CI, c) DTS and d) DDTS. Circles indicate synthetic calcium.

Table 1. Calculated CNR, with improvement compared to TI in brackets, for the four PLs shown in Fig. 3

	TI (a)	CI (b)	DTS (c)	DDTS (d)
PL1: CNR (Imp.)	0.43 (-%)	1.10 (156%)	4.69 (990%)	4.77 (1009%)
PL2: CNR (Imp.)	0.25 (-%)	0.28 (12%)	3.67 (1368%)	5.06 (1924%)
PL3: CNR (Imp.)	0.56 (-%)	0.63 (12%)	4.50 (703%)	4.61 (723%)
PL4: CNR (Imp.)	0.64 (-%)	1.33 (108%)	6.37 (895%)	6.25 (877%)
Average Imp.	**-**	**72%**	**989%**	**1133%**

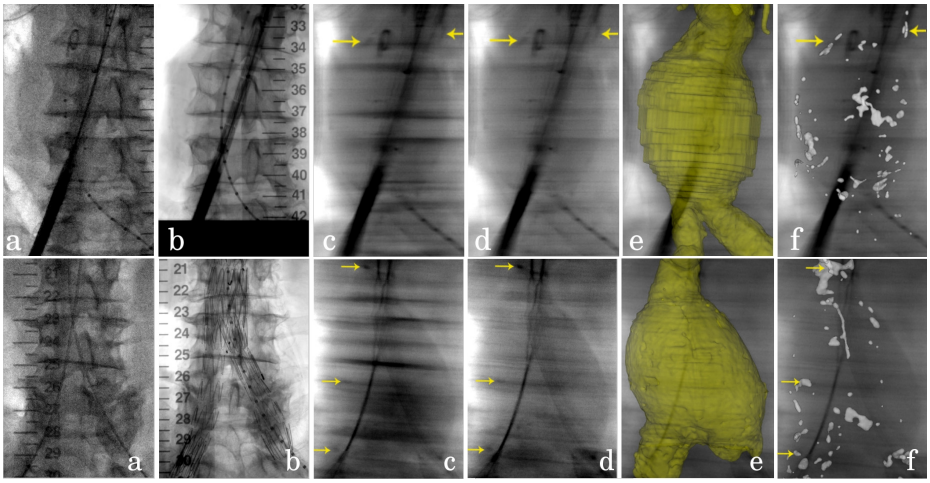

Fig. 4. Patient 1 (top) and patient 2 (bottom) results: (a) TI, (b) CI, (c) DTS, (d) DDTS, (e) AAA overlay and (f) calcification overlay into the DDTS slice. Arrows indicate calcium deposits.

5 Discussion and Conclusions

The development of novel imaging technologies capable of near-real-time visualisation of soft-tissue structures in the interventional suite is challenging. Short acquisition and reconstruction times, low radiation dose and minimal interruption to the clinical workflow are key requirements for an effective interventional

modality. We have presented a novel technique, "interventional digital tomosynthesis", which can be directly implemented on existing fluoroscopy systems. The small C-arm sweep of $\pm 20°$ takes a fraction of the image acquisition time and radiation dose compared to CBCT, and causes very little disruption to the clinical workflow.

Our method was able to enhance clinically important structures situated on a curved surface. These structures could provide additional spatial information during interventions, offering surgeons an increased guidance precision and confidence. Contrast usage would be reduced compared to the techniques currently used to visualise the aorta, which require injection of iodinated contrast.

The preoperative CT overlays (Fig. 4.(e&f)) needed manual adjustment to accurately match our DDTS images. This was due to anatomical deformation occurring during intervention caused by the stiff interventional instruments [7]. This shows a potential application for our interventional DTS: to provide additional information to update overlays from an image guided surgery system enabling more accurate representation of the intraoperative scene.

In summary, a novel method of interventional DTS has been presented. The method employs a 2D-3D registration algorithm to enable production of DTS slices using standard interventional equipment, with much reduced out-of-plane clutter and on a patient tailored reconstruction surface. Results from a phantom and two patients show the method's ability to automatically enhance structures of clinical interest.

References

1. Bachar, G., Barker, E., Nithiananthan, S., Chan, H., Daly, M., Irish, J., Siewerdsen, J.: Three-dimensional tomosynthesis and cone-beam computed tomography: an experimental study for fast, low-dose intraoperative imaging technology for guidance of sinus and skull base surgery. The Laryngoscope 119(3), 434–441 (2009)
2. Bachar, G., Siewerdsen, J., Daly, M., Jaffray, D., Irish, J.: Image quality and localization accuracy in C-arm tomosynthesis-guided head and neck surgery. Med. Phys. 34, 4664 (2007)
3. Dobbins III, J.: Tomosynthesis imaging: at a translational crossroads. Med. Phys. 36(6), 1956–1967 (2009)
4. Dobbins III, J., Godfrey, D.: Digital x-ray tomosynthesis: current state of the art and clinical potential. Phys. Med. Biol. 48(19), 65–106 (2003)
5. Gang, G., Tward, D., Lee, J., Siewerdsen, J.: Anatomical background and generalized detectability in tomosynthesis and cone-beam CT. Med. Phys. 37(5) (2010)
6. Jaffray, D., Siewerdsen, J., Wong, J., Martinez, A., et al.: Flat-panel cone-beam computed tomography for image-guided radiation therapy. Int. J. Radiat. Oncol. Biol. Phys. 53(5), 1337–1349 (2002)
7. Penney, G., Varnavas, A., Dastur, N., Carrell, T.: An image-guided surgery system to aid endovascular treatment of complex aortic aneurysms: Description and initial clinical experience. In: Taylor, R.H., Yang, G.-Z. (eds.) IPCAI 2011. LNCS, vol. 6689, pp. 13–24. Springer, Heidelberg (2011)
8. Wallace, M., Kuo, M., Glaiberman, C., Binkert, C., Orth, R., Soulez, G.: Three-dimensional C-arm cone-beam CT: applications in the interventional suite. J. Vasc. Interv. Radiol. 19(6), 799–813 (2008)